Transmission Capacity of Wireless *Ad Hoc* Networks With Successive Interference Cancellation

Steven P. Weber, *Member, IEEE*, Jeffrey G. Andrews, *Senior Member, IEEE*, Xiangying Yang, *Member, IEEE*, and Gustavo de Veciana, *Senior Member, IEEE*

***Abstract*—The transmission capacity (TC) of a wireless *ad hoc* network is defined as the maximum spatial intensity of successful transmissions such that the outage probability does not exceed some specified threshold. This work studies the improvement in TC obtainable with successive interference cancellation (SIC), an important receiver technique that has been shown to achieve the capacity of several classes of multiuser channels, but has not been carefully evaluated in the context of *ad hoc* wireless networks. This paper develops closed-form upper bounds and easily computable lower bounds for the TC of *ad hoc* networks with SIC receivers, for both perfect and imperfect SIC. The analysis applies to any multiuser receiver that cancels the K strongest interfering signals by a factor $z \in [0,1]$. In addition to providing the first closed-form capacity results for SIC in *ad hoc* networks, design-relevant insights are made possible. In particular, it is shown that SIC should be used with direct sequence spread spectrum. Also, any imperfections in the interference cancellation rapidly degrade its usefulness. More encouragingly, only a few—often just one—interfering nodes need to be canceled in order to get the vast majority of the available performance gain.**

***Index Terms*—*Ad hoc* networks, successive interference cancellation, transmission capacity (TC).**

I. Introduction

UNDERSTANDING the performance limits of decentralized ("*ad hoc*") wireless networks is a subject of much recent work. Due to the difficulty of directly analyzing the capacity of an unconstrained n-node network [1], most recent work has followed the lead of the seminal work of Gupta and Kumar [2] and studies how the capacity scales with n under a variety of different modeling and implementation scenarios [3]–[8].

In contrast, other recent work by Baccelli *et al.*, [9], [10], Chan and Hanly [11], and the present authors [12] adopts a stochastic geometric approach for studying the performance of *ad hoc* networks. Stochastic geometric approaches for wireless networks can be traced back to seminal work by Sousa and Silvester [13], [14]. In particular, [12] develops an analytical framework termed the *transmission capacity* (TC), the maximum allowable spatial density λ of transmitters in an *ad hoc* network, as a function of various parameters like transmit distance and required signal-to-interference-plus-noise ratio (SINR), such that a specified outage probability ϵ is met. Using this framework, TC bounds are found for frequency hopping (FH) and direct sequence (DS) code-division multiple access (CDMA) (with a matched filter receiver) with the conclusion that in contrast to centralized networks, FH is significantly superior in an *ad hoc* network. In particular, our results predict a performance improvement on the order of $M^{1-\frac{2}{\alpha}}$, where M is the spreading factor and $\alpha > 2$ is the path loss exponent. The conclusion is that it is preferable to *avoid* interference by FH rather than to *suppress* it through random spreading. Intuitively, most outages are a result of an interfering node close to a receiver, and due to the strength of this interference, these occurrences are better addressed by using different channels as opposed to receivers trying to suppress the interference.

A. Successive Interference Cancellation

Since outages are predominantly caused by just a few nearby interfering users, an appealing alternative to interference avoidance (which consumes resources such as time or frequency slots) is interference cancellation. In fact, it is well known that the matched-filter receiver considered in [12], while dominant in commercial CDMA systems, is dramatically suboptimal in theory relative to multiuser receivers, particularly in the presence of widely variant receiver powers [15], [16]. In general, multiuser receivers achieve a performance gain by exploiting the structure of the multiuser interference, rather than just treating it as wideband noise. A particularly interesting type of multiuser detection is successive interference cancellation (SIC), first suggested in [17]; one form of SIC is shown in Fig. 1. The key idea of SIC is that users are decoded sequentially, with the receiver canceling interference after each user. For example, the decoded data for the first user is re-encoded and by using accurate channel knowledge, can be made to very closely resemble its *received* signal. Hence, it can be subtracted out of the composite received signal, and the second user to be decoded experiences less interference than it would have otherwise. The process can be continued for an arbitrary number of users.

In addition to its simplicity and amenability to implementation [18], SIC is well justified from a theoretical point of view. Simple successive interference cancellation implementation with suboptimal coding was shown to nearly achieve the Shannon capacity of multiuser additive white Gaussian noise (AWGN) channels, assuming accurate channel estimation and a

Manuscript received August 19, 2005; revised August 23, 2006. This work was supported in part by the National Science foundation under Grants 0635003 (Weber), 0634979 (Andrews), and 0435307 (de Veciana), as well as the DARPA IT-MANET Program under Grant W911NF-07-1-0028 (Andrews and Weber).

S. Weber is with the Department of Electrical and Computer Engineering, Drexel University, Philadelphia, PA 19104-2875 USA (e-mail: sweber@ece.drexel.edu).

J. G. Andrews and G. de Veciana are with the Department of Electrical and Computer Engineering, The University of Texas at Austin, Austin, TX 78712-0240 USA (e-mail: jandrews@ece.utexas.edu).

X. Yang was with The University of Texas at Austin, Austin, TX 78712 USA. He is now with Intel Corporation, Portland, OR 97229-9217 USA (e-mail: yangxy@gmail.com).

Communicated by M. Médard, Associate Editor for Communications.

Digital Object Identifier 10.1109/TIT.2007.901153

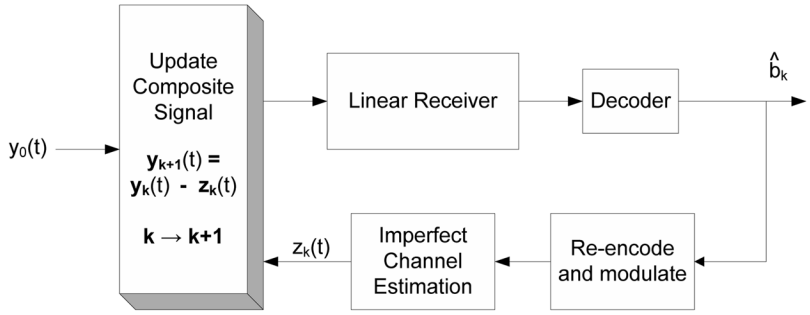

Fig. 1. Block diagram of successive interference cancellation.

large spreading factor [19]. Other more recent work has proven that SIC with single-user decoding in fact achieves the Shannon capacity region boundaries for both the broadcast (downlink) and multiple-access (uplink) multiuser channel scenarios [20], [21], as well-summarized in [22]. Quantifying SIC's benefit in *ad hoc* networks is naturally more problematic, but initial evidence for its promise is given in [23]. Since it is well suited to asynchronous signals of unequal powers [24], and has much lower complexity than most other multiuser receivers, it appears to be a natural fit for a wireless *ad hoc* networks from the standpoint of both theory and practice.

Accurately modeling and analyzing SIC in *ad hoc* networks requires some nontrivial extensions from centralized networks. For instance, it has been shown that a particular (unequal) distribution of received powers is needed for SIC systems to perform well, especially when the interference cancellation is imperfect [25], [26]. Achieving such a distribution at each receiver in an *ad hoc* network is impossible due to the random spatial characteristics of the network. Related to this, to be realistic it should be assumed that only strong signals can be canceled, hence, at any given location in the network, only the nearby interferers are cancelable. In order to accurately quantify SIC's performance in *ad hoc* networks, Section II will develop a realistic (but analytically tractable) model in view of such considerations.

B. Main Results and Insights

The principal contribution of this paper are closed-form (and reasonably tight) upper and lower bounds on the TC for wireless *ad hoc* networks for imperfect successive interference cancellation, where a residual fraction z of the interference is left after each stage. These results are obtained for a stochastic geometric model of SIC which approximates the performance of an actual SIC receiver. Results without SIC and for perfect SIC are first derived for pedagogical purposes, and naturally are the special (and analytically simpler) case where z goes to 0. Prior results for wireless networks without SIC are also a special case where z goes to 1. The model and results are general enough that any multiuser receiver structure with residual cancellation error z on the K closest nodes would be covered by our analysis.

The derivations and main results are organized as follows. Section III presents three general theorems that are used as building blocks. Sections IV, V, and VI then use those theorems to develop the upper and lower bounds and both outage probability and TC. Section IV states for the case of no SIC Lemma 1 and Lemma 2, which, respectively, are the upper (lower) and lower (upper) bounds on TC (outage probability). Similarly, Section V comprises Lemmas 3 and 4 for the case of perfect SIC, and Section VI comprises Lemmas 5 and 6 for the case of imperfect SIC. The upper bounds on TC are closed form. The lower bounds are not, but only require a straightforward computation to be evaluated numerically.

The following are the key insights that can be gleaned from our theoretical analysis. Note that many of these conclusions are distinct from those for cellular/centralized networks.

- *SIC is useful primarily in conjunction with spread spectrum*. Due to the network geometry, the largest gains from using SIC are when the target received signal-to-interference ratio (SIR) $\beta < 1$. In fact, for imperfect SIC, no gain is seen unless $z\beta < 1$ because the farther away interferers (that are not cancelable) can still cause an outage, and the nearby interferers are not sufficiently suppressed. Low target SIRs are viable only in the case of spread-spectrum signaling, where a spreading gain of M allows the received SIR to decrease by a factor of about M while maintaining a reasonable communication fidelity.
- *The interference cancellation must be very accurate*. Most of the performance improvement obtainable through SIC is gained by canceling just the single transmitter with the largest interference level; canceling additional transmitters carries a negligible benefit unless the cancellation is *very* accurate, i.e., $z \rightarrow 0$. This is again due to the network geometry: even the residual interference of close-by interferers can often be the dominant interference source.
- *The network density largely determines the efficacy of SIC*. When the network is too dense, the receiver becomes overwhelmed. When the network is sparse, SIC's effectiveness is governed largely by the residual interference z. There exists a density "sweet spot" for SIC where the TC increases additively with the number of cancelable nodes K.

The rest of this paper is organized as follows. Section II introduces the mathematical model and notation. Section III gives general results on the lower and upper bounds on the outage probability and TC. Sections IV, V, and VI apply these general results to the specific cases of no interference cancellation, perfect cancellation, and imperfect cancellation, respectively. Section VII presents numerical and simulation results and Section VIII contains a conclusion. The proofs of the three theorems from Section III are placed in the Appendix.

II. Mathematical Model

A. Wireless Ad Hoc Network

Our model employs a homogeneous Poisson point process (PPP) $\Phi = \{X_i, i \in \mathbb{N}\}$ on the plane $\mathbb{R}^2$ to represent the locations of all nodes transmitting at some time instant t. Let $|X_i|$ represent the distance from the location of transmitter i to the origin. The PPP model for terminal positions has proven very accurate for CDMA cellular networks, and has produced analytical calculations for blocking probability that come within a few percent of actual blocking rates for service providers [27]. The spatial density of the point process is denoted by λ, giving the average number of nodes attempting transmissions per unit area

$$\frac{\mathbb{E}[|\Phi \cap A|]}{|A|} = \lambda, \qquad A \subset \mathbb{R}^2. \tag{1}$$

In prior work [12], we considered two models for power control: i) all transmitters use the same transmission power, ρ, and all transmission distances are over the same distance r, and ii) transmitters vary their transmission power over variable distances to achieve a specified receive power. In that work, we demonstrated the TC scales very similarly for both models, so for analytical simplicity we use the first model in this paper. To emphasize: we assume a constant transmission power of ρ, and that each transmitter is separated from its next hop intended receiver by a distance of r meters.

Our channel model considers only path loss attenuation effects and ignores additional channel effects such as shadowing and fast fading. Although these random channel effects may be considerable particularly in the context of opportunistic scheduling, they do not have an especially large effect on capacity scaling in the absence of channel information and opportunistic scheduling [7], [10], [28], [29]. In particular, our channel model is

$$h(|x|) = \begin{cases} |x|^{-\alpha}, & |x| > 1 \\ 0, & \text{else} \end{cases} \tag{2}$$

where ρ is the (normalized to $|x| = 1$) transmit power, $\alpha > 2$ is the path loss exponent, and $|x|$ is the distance from the transmitter at location $x \in \mathbb{R}^2$ to the reference receiver at the origin. The assumption that $h(|x|) = 0$ for all x in $b(o, 1)$ is a mathematically convenient way to deal with the physically unreasonable singularity that arises at the origin under power law attenuation. We denote the SIR threshold required for successful transmission as β. One additional simplification employed in this paper relative to [12] is that here we will assume the ambient (thermal) noise power is negligibly small, which is almost always the case in interference-limited wireless networks. The spatial interference model in this paper is general enough to include any randomly located radio frequency (RF) devices that are generating moderate levels of in-band interference; they do not need to be an explicit part of the *ad hoc* network *per se*. The noiseless assumption is made to simplify the analysis and resulting expressions, and is verified to be reasonable via simulation.

Shot noise processes were introduced by Schottky [30] in 1918 to represent the cumulative effect at time t of a sequence of shocks appearing at random times $T_i < t$, each attenuated in time by an impulse function $h(|t - T_i|)$. Lowen and Teich provide a thorough characterization of the properties of power law shot noise processes [31], i.e., when $h(|x|) = |x|^{-\alpha}$. *Spatial* shot noise processes capture the cumulative effect at location x of a set of random shocks appearing at random locations X_i, where the impulse function $h(|X_i - x|)$ gives the attenuation in space. It has long been recognized that the cumulative interference seen by a receiver in a wireless network is a spatial shot noise process, where the impulse function is determined by the channel model, e.g., [14].

Definition 1: The *normalized aggregate interference* is the shot noise experienced by the reference receiver at the origin

$$Y = \sum_{i \in \Phi} |X_i|^{-\alpha} \mathbf{1}_{\{|X_i| > 1\}}. \tag{3}$$

A beneficial consequence of the Poisson assumption is that, by Slivnyak's theorem [32], the client-average outage probability may be found by evaluating the SIR seen by a receiver located at the origin. Intuitively, the distribution of the point process is unaffected by the addition of a receiver at the origin, and this receiver is "typical" in the sense that evaluating the performance seen at the origin gives the client-average performance over all receivers. Measuring the performance at the origin is often termed the Palm measure, and in keeping with standard notation we will denote probability and expectation of functionals of Φ evaluated at the origin by $\mathbb{P}^0$ and $\mathbb{E}^0$, respectively. The outage probability $p(\lambda)$ is the probability that the SIR seen by the typical receiver at the origin is insufficient. The following definition establishes that the outage probability may be expressed in terms of the complementary cumulative distribution function (CCDF) of the shot noise.

Definition 2: The *outage probability* is the probability the SIR experienced by the reference receiver at the origin is below the threshold β

$$\begin{aligned} p(\lambda) &= \mathbb{P}^0(\text{SIR} < \beta) \\ &= \mathbb{P}^0\left(\frac{\rho r^{-\alpha}}{\rho Y} < \beta\right) \\ &= \mathbb{P}^0\left(Y > \frac{1}{\beta r^{\alpha}}\right). \end{aligned} \tag{4}$$

Note since we have neglected ambient noise, the outage probability is independent of the transmission power ρ. If the typical outage probability must be below a specified threshold ϵ, then it is natural to inquire as to the maximum density of attempted transmissions that will respect that bound. The optimal contention density $\lambda(\epsilon)$ formalizes this notion: it is the maximum intensity of attempted transmissions such that the typical node will experience an outage probability no larger than ϵ. The TC $c(\epsilon)$ is the corresponding maximum spatial throughput, found by multiplying by the achievable data rate b, and thinning the attempted transmissions by the success probability $(1 - \epsilon)$.

Definition 3: The *optimal contention density*, $\lambda(\epsilon)$, is the maximum spatial density of nodes that can contend for the

channel subject to the constraint that the typical outage probability is less than ϵ for some $\epsilon \in (0,1)$:

$$\lambda(\epsilon) = \sup\{\lambda : p(\lambda) \leq \epsilon\}. \tag{5}$$

Note that the TC $\lambda(\epsilon)$ is monotone increasing in ϵ; this is a consequence of the fact that less stringent quality of service (QoS) requirements (higher ϵ) permit a greater degree of spatial reuse.

Definition 4: The *transmission capacity* $c(\epsilon)$ is the density of successful transmissions resulting from the optimal contention density, multiplied by the achievable data rate b of a typical (i.e., average) successful (not in outage) transmission

$$c(\epsilon) = b(1-\epsilon)\lambda(\epsilon). \tag{6}$$

The TC has units of bits per second per Hertz per area, or area spectral efficiency. As in previous work [12], for simplicity in this paper it is assumed henceforth that $b = 1$, so the focus is on quantifying the number of successful transmissions, rather than on the data rate of those transmissions. We note in general that $b \propto \log(1+\beta)$. Fixing b is appropriate in the context of this paper since the motivation for multiuser receivers is to increase the number of simultaneous users. The general definition allows other transmission or receiver schemes to increase the data rate for a fixed number of users and be credited appropriately in the TC framework.

The key idea underlying our lower and upper bounds on outage probability and TC is that of near and far fields.

Definition 5: The *near field* $F_n \subset \mathbb{R}^2$ consists of locations in space such that a single node at that location is capable of generating sufficient interference to cause an outage for the reference receiver at the origin. The *near-field interferers* $\Phi_n = \Phi \cap F_n$ are nodes in the near field. The *near-field interference* Y_n is the interference generated by the near-field nodes.

Definition 6: The *far field* $F_f = \mathbb{R}^2 \setminus (b(o,1) \cup F_n)$ consists of locations in space such that a single node at that location is not capable of generating sufficient interference to cause an outage for the reference receiver at the origin. The *far-field interferers* $\Phi_f = \Phi \setminus \Phi_n$ are nodes in the far field. The *far-field interference* $Y_f = Y - Y_n$ is the interference generated by the far-field nodes.

The terms near and far field should not be confused with their use in the channel modeling literature. For convenience, we summarize in Table I most of the notation used in the paper.

TABLE I
SUMMARY OF MATHEMATICAL NOTATION

$x \wedge y$	$\min\{x, y\}$
$a(o, r_1, r_2)$	$\{x : r_1 \leq \lvert x\rvert \leq r_2\}$, i.e., an annulus between r_1 and r_2
α	path loss exponent ($\alpha > 2$)
$b(o, r)$	$\{x : \lvert x\rvert \leq r\}$, i.e., a ball of radius r centered at origin
β	target (required) SIR
$c(\epsilon)$	transmission capacity, $c(\epsilon) = \lambda(\epsilon)(1-\epsilon)$
$\sqrt{\frac{K}{\pi\lambda}} \wedge r$	cancellation radius
ϵ	required outage probability, i.e., $p(\lambda) \leq \epsilon \in (0,1)$
F_n, F_f	the near and far fields: $F_n \cup F_f = \mathbb{R}^2 \setminus b(o,1)$
K	maximum number of cancelled users, $K \in \mathbb{N}$
λ	transmission density, intensity of PPP Φ
$\lambda(\epsilon)$	optimal contention density, obeys $p(\lambda(\epsilon)) = \epsilon$
$p(\lambda)$	outage probability $\mathbb{P}^0(\mathrm{SIR} \leq \beta)$
$\Phi = \{X_i\}$	the PPP of intensity λ denoting transmitter locations
Φ_n, Φ_f	transmitters in the near and far fields
r	transmit distance
ρ	transmit power
Y	normalized aggregate interference seen at the origin
Y_n, Y_f	interference from the near and far field transmitters
z	residual interference after cancellation, ($z \in [0,1]$)
iSIC	specifies imperfect SIC, i.e., $K > 0$ and $z \in (0,1)$
nSIC	specifies no SIC, i.e., $z = 1$ or $K = 0$
pSIC	specifies perfect SIC, i.e., $K > 0$ and $z = 0$

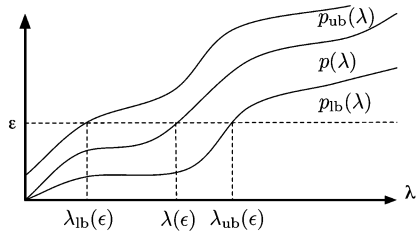

Fig. 2. Lower and upper bounds on the optimal contention density $\lambda_{\mathrm{lb}}(\epsilon) \leq \lambda(\epsilon) \leq \lambda_{\mathrm{ub}}(\epsilon)$ are obtained by inverting lower and upper bounds on the outage probability $p_{\mathrm{lb}}(\lambda) \leq p(\lambda) \leq p_{\mathrm{ub}}(\lambda)$.

III. General Results

In this section, we derive lower and upper bounds on the outage probability and TC using the concept of near- and far-field regions and interferers. These general bounds will be applied to the three cases of no SIC, perfect SIC, and imperfect SIC in the sequel.

Theorem 1: A lower bound on the outage probability is given by

$$p_{\mathrm{lb}}(\lambda) = 1 - \exp\{-\lambda\nu(F_n)\} \tag{7}$$

where $\nu(A)$ is the area of the set $A \subset \mathbb{R}^2$. Provided $\nu(F_n) > 0$, this lower bound may be used to obtain an upper bound on the TC by solving $p_{\mathrm{lb}}(\lambda) = \epsilon$ for λ.

The proof is found in the Appendix. The theorem establishes a lower bound that depends upon the *area* of the near field. In essence, the result follows from the facts that i) the outage probability due to aggregate interference exceeds the outage probability due to near-field interference, and ii) by construction, the event of a near-field outage is the same as the event of there being one or more near-field interferers. The probability of one or more near-field interferers is a geometric quantity: it is one minus the void probability for a Poisson point process, which may expressed in terms of its intensity and the area of the near field. The authors establish that this lower bound is asymptotically optimal as $y \doteq \frac{1}{\beta r^\alpha} \to \infty$ in [29].

The lower bound on the outage probability yields an upper bound on the optimal contention density, as illustrated in Fig. 2. In the simple case, where the near field is independent of λ, the upper bound on the optimal contention density is

$$\lambda_{\mathrm{ub}}(\epsilon) = \frac{-\log(1-\epsilon)}{\nu(F_n)} \tag{8}$$

however, we will in general consider models where the appropriate near-field does depend on λ.

The upper bound on the outage probability is based on the Chernoff bound on the far-field interference, combined with the

lower bound given above. The Chernoff bound on the far-field outage probability is given in Theorem 2 below, for a general interference model which includes regions of partially canceled nodes. We let $a(o, r_1, r_2)$ denote the annulus with radii $r_1 < r_2$ centered at the origin, o. The interference model assumed in the theorem is chosen to be able to calculate the far-field outage probability under the imperfect SIC model discussed in Section VI.

Theorem 2: Consider a far field consisting of two bands $a(o, s, t)$ and $a(o, u, \infty)$ for $1 \leq s \leq t \leq u$. Suppose interference generated by nodes in $a(o, s, t)$ is partially canceled by a factor $z \in [0, 1]$, while interference generated by nodes in $a(o, u, \infty)$ is not canceled. The Chernoff bound on the probability of outage generated by far field interference is

$$\mathbb{P}\left(Y_f > \frac{1}{\beta r^\alpha}\right) \leq \exp\{-\Lambda^*(F_f)\} \tag{9}$$

where

$$\Lambda^*(F_f) = \sup_{\theta \geq 0} \left\{ \frac{\theta}{\beta r^\alpha} - 2\pi\lambda \times \left[\int_s^t x \left(\mathrm{e}^{\theta z x^{-\alpha}} - 1 \right) \mathrm{d}x + \int_u^\infty x \left(\mathrm{e}^{\theta x^{-\alpha}} - 1 \right) \mathrm{d}x \right] \right\}. \tag{10}$$

This bound holds for all

$$\lambda < \frac{(\alpha - 2)}{2\pi\beta r^\alpha} \left(u^{2-\alpha} + z(s^{2-\alpha} - t^{2-\alpha}) \right)^{-1}. \tag{11}$$

The proof is found in the Appendix. The function inside the supremum is convex in θ (since $\Lambda^*(F_f)$ is a Chernoff bound rate function), and as such the optimal θ is the solution of

$$\frac{1}{2\pi\lambda\beta r^\alpha} = z \int_s^t x^{1-\alpha} \mathrm{e}^{\theta z x^{-\alpha}} \mathrm{d}x + \int_u^\infty x^{1-\alpha} \mathrm{e}^{\theta x^{-\alpha}} \mathrm{d}x. \tag{12}$$

This is found by differentiating with respect to θ and setting the resulting expression equal to zero. The constraint on λ is found by solving $\frac{1}{\beta r^\alpha} > \mathbb{E}[Y_f]$ for λ, where

$$\mathbb{E}[Y_f] = \frac{2\pi\lambda}{\alpha - 2}(u^{2-\alpha} + z(s^{2-\alpha} - t^{2-\alpha})) \tag{13}$$

which is easily computed from Campbell's theorem [32]. With the Chernoff bound on the far-field interference in hand, we again apply the near- and far-field paradigm to obtain an upper bound on the outage probability.

Theorem 3: An upper bound on the outage probability is given by

$$p_{\mathrm{ub}}(\lambda) = 1 - (1 - \exp\{-\Lambda^*(F_f)\}) \exp\{-\lambda\nu(F_n)\} \tag{14}$$

where $\mathrm{e}^{-\Lambda^*(F_f)}$ is the Chernoff upper bound on the probability of a far-field-induced outage event from Theorem 2. Provided $\Lambda^*(F_f) > 0$, this upper bound may be used to obtain a lower bound on the TC by solving $p_{\mathrm{ub}}(\lambda) = \epsilon$ for λ.

The proof is found in the Appendix. The upper bound is more unwieldy than the lower bound as the rate function in the Chernoff upper bound requires computation of the optimal value of θ. Although this is straightforward to do numerically, it is difficult to say anything qualitatively about how the optimal θ depends upon the parameters s, t, u, z. As such, we will base our discussion of the structural properties of the model on the lower bound on outage probability. The lower bound on the TC is obtained from the upper bound on outage probability as illustrated in Fig. 2.

IV. No Successive Interference Cancellation

First, we give lower and upper bounds on the outage probability and the TC for the base case where no interference cancellation is applied, denoted as nSIC to mean "no SIC." These results are obtainable from our earlier work [12] with a spreading factor $M = 1$. To apply the general results of the previous section it is necessary to identify the near and far fields.

Lemma 1: Without SIC, the lower bound on outage probability is

$$p_{\mathrm{lb}}^{\mathrm{nSIC}}(\lambda) = 1 - \exp\{-\lambda\pi(\beta^{\frac{2}{\alpha}} r^2 - 1)\}. \tag{15}$$

The upper bound on the TC is

$$c_{\mathrm{ub}}^{\mathrm{nSIC}}(\epsilon) = \frac{-(1 - \epsilon)\log(1 - \epsilon)}{\pi(\beta^{\frac{2}{\alpha}} r^2 - 1)}. \tag{16}$$

Proof: The near field is computed by finding the largest distance such that a single interfering node at that distance can by itself generate sufficient interference for the reference receiver at the origin to cause an outage. Using the specified path loss attenuation channel model, we can solve for the near-field radius as

$$\frac{\rho r^{-\alpha}}{\rho d^{-\alpha}} = \beta \Rightarrow d = \beta^{\frac{1}{\alpha}} r. \tag{17}$$

The near field without SIC is therefore $F_n^{\mathrm{nSIC}} = a(o, 1, \beta^{\frac{1}{\alpha}} r)$. The area associated with the near field is $\nu(F_n^{\mathrm{nSIC}}) = \pi(\beta^{\frac{2}{\alpha}} r^2 - 1)$. □

Lemma 2: Without SIC, the far field is $F_f^{\mathrm{nSIC}} = a(o, \beta^{\frac{1}{\alpha}} r, \infty)$ which corresponds to setting $s = t = u = \beta^{\frac{1}{\alpha}} r$ in Theorem 2. The upper bound on outage probability is

$$p_{\mathrm{ub}}^{\mathrm{nSIC}}(\lambda) = 1 - \left(1 - \exp\left\{-\Lambda^*\left(F_f^{\mathrm{nSIC}}\right)\right\}\right) \times \exp\left\{-\lambda\nu\left(F_n^{\mathrm{nSIC}}\right)\right\}. \tag{18}$$

The corresponding lower bound on the TC is obtained by solving $p_{\mathrm{ub}}^{\mathrm{nSIC}}(\lambda) = \epsilon$ for λ.

Proof: Note that for $\beta > 1$, the near field extends beyond r, the transmission radius, while for $\beta < 1$, the near field has a smaller radius than the transmission radius. Looking at the definition of the parameters s, t, u, z in Theorem 2, it is clear that the appropriate selection for the parameters is $s = t = u = \beta^{\frac{1}{\alpha}} r$ and $z = 1$ (although when $s = t$ the dependence on z vanishes). □

In our previous work [12], we employed both Markov and Chebychev inequalities to obtain the upper bound on the outage

probability. This approach has the strength that it yields closed-form expressions for the upper bound on outage probability (and hence closed-form expressions for the lower bound on the TC). Applying the Markov and Chebychev bounds for the more complicated models with perfect and imperfect interference cancellation, however, is much more involved, and often closed-form expressions are not available. Moreover, the Markov and Chebychev bounds are often not as tight as the Chernoff bound. For these reasons, we present all our outage probability upper bounds using Chernoff bounds.

V. Perfect Successive Interference Cancellation

Successive interference cancellation allows users to be decoded one at a time, and then subtracted out from the composite received signal in order to improve the performance of subsequently decoded users. In practice, this corresponds to decoding the strongest user first, since it will experience the best SIR and hence be the most accurately decoded, which is a prerequisite for accurate interference cancellation. More generally, by similar reasoning, users should be decoded in order of their received powers [19], [33] (even though this is not always the preferred order from an information-theoretic viewpoint [22]). In an *ad hoc* network with a path loss channel model, this corresponds to canceling the interference from nodes closer to the receiver than the desired transmitter.

An accurate characterization of the performance gains due to SIC should be based on a plausible interference cancellation scenario; otherwise, the results can in fact be quite optimistic and misleading. Particularly, an accurate model would capture that an SIC-equipped receiver is able to reduce the interference power of up to K nearest interfering nodes by a factor $1-z$ (i.e., residual interference power of z), assuming these nodes are closer than our desired transmitter. However, it is difficult to work with this exact model in a mathematical framework, since it requires a characterization of the joint distribution of the distances of the K nodes nearest to the origin, see [34].

Instead of pursuing this exact approach, we utilize a closely related SIC model that is more amenable to analysis. In particular, define the *cancellation region* as the set of locations around the reference receiver such that the receiver is capable of reducing the interference power by z of any and all transmitters located in that region. The cancellation region will be a disk, and the radius of the disk is chosen so that there are *on average* K interfering nodes in the cancellation region. Since the average number of points in a Poisson process of intensity λ falling in a circle of radius d is $\lambda\pi d^2$, we find the appropriate cancellation radius is $\sqrt{\frac{K}{\pi\lambda}}$ by solving $\lambda\pi d^2 = K$ for d. It is normally only feasible to cancel the interference from those nodes whose interference power measured at the receiver exceeds the signal power. In the absence of channel fades, our deterministic path loss model implies that received interference power levels depend only upon the distance of the interferer from the origin. It follows that only nodes in $b(o,r)$ are eligible for cancellation, where r is the transmission radius between transmitters and their intended receivers. Combining these two concepts leads to a cancellation radius of $\sqrt{\frac{K}{\pi\lambda}} \wedge r$.

Definition 7: A (K,z) *SIC receiver* operating in a network with a transmission density of λ is capable of reducing the interference power by a factor $1-z$ for all interfering nodes within distance $\sqrt{\frac{K}{\pi\lambda}} \wedge r$. An *imperfect SIC receiver* has a cancellation effectiveness of $z \in (0,1)$, while a *perfect SIC receiver* has cancellation effectiveness of $z = 0$ (no residual interference for cancelled nodes).

Note that setting $z = 1$ or $K = 0$ recovers the no SIC model covered previously. The cancellation radius is r for $\lambda \leq \frac{K}{\pi r^2}$, and is decreasing in λ for $\lambda > \frac{K}{\pi r^2}$. Viewed as a function of λ, the cancellation radius is independent of λ for λ small, and is decreasing in λ for λ large. Intuitively, if λ is small then there are few interferers on average, and the cancellation effectiveness is limited by the requirement that interference power exceed signal power. If λ is large, on the other hand, there are many nodes to select from, and the cancellation effectiveness is limited by the requirement that at most K signals may be processed.

To apply the general results for the perfect SIC model we must identify the appropriate near- and far-field regions. Please see Fig. 3. The figure shows the near-field annulus for each possible λ, for the cases $\beta > 1$ (top) and $\beta < 1$ (bottom). Recall that in studying the no SIC model it was determined that the near field consisted of the annulus $a(o,1,\beta^{\frac{1}{\alpha}}r)$. The near field under perfect SIC is simply all locations lying in the no SIC near field but outside the cancellation region. When $\beta > 1$, the near-field radius is always larger than the cancellation radius, and so the near field is always well defined. When $\beta < 1$, however, the near field is empty for all

$$\lambda < \frac{K}{\pi\beta^{\frac{2}{\alpha}}r^2}$$

(this expression is obtained by solving $\beta^{\frac{1}{\alpha}}r = \sqrt{\frac{K}{\pi\lambda}}$ for λ). The absence of a near field leads to a trivial lower bound on outage probability of 0, and a trivial upper bound on the TC of infinity. The fact that the cancellation region is a superset of the near field for this region means that an outage can only occur through the confluence of far-field interferers. The following theorem applies the results from Fig. 3 to the general results on the lower bound in Theorem 1; the proof is immediate from the figure.

Lemma 3: Consider perfect SIC. For $\beta > 1$, the lower bound on the outage probability is

$$p_{\mathrm{lb}}^{\mathrm{pSIC}}(\lambda) = \begin{cases} 1 - \exp\left\{-\lambda\pi r^2\left(\beta^{\frac{2}{\alpha}} - 1\right)\right\}, & \lambda < \frac{K}{\pi r^2} \\ 1 - \exp\left\{-\lambda\pi\beta^{\frac{2}{\alpha}}r^2 + K\right\}, & \text{else.} \end{cases} \tag{19}$$

and the upper bound on TC is

$$c_{\mathrm{ub}}^{\mathrm{pSIC}}(\epsilon) = \begin{cases} \frac{-(1-\epsilon)\log(1-\epsilon)}{\pi r^2(\beta^{\frac{2}{\alpha}}-1)}, & \epsilon < 1 - \mathrm{e}^{-(\beta^{\frac{2}{\alpha}}-1)} \\ \frac{(1-\epsilon)(-\log(1-\epsilon)+K)}{\pi\beta^{\frac{2}{\alpha}}r^2}, & \text{else.} \end{cases} \tag{20}$$

For $\beta \leq 1$, the lower bound on the outage probability is

$$p_{\mathrm{lb}}^{\mathrm{pSIC}}(\lambda) = \begin{cases} 0, & \lambda < \frac{K}{\pi\beta^{\frac{2}{\alpha}}r^2} \\ 1 - \exp\left\{-\lambda\pi\beta^{\frac{2}{\alpha}}r^2 + K\right\}, & \text{else.} \end{cases} \tag{21}$$

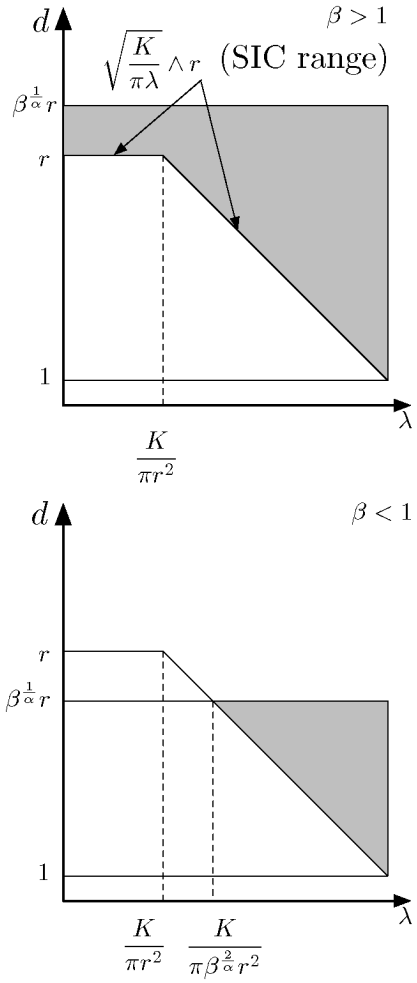

Fig. 3. Illustration of the near-field region (shaded) for the perfect cancellation model. The x-axis is the spatial density of attempted transmissions (λ) and the y-axis is the distance from the origin d. The shape of the near field depends upon whether $\beta > 1$ (top) or $\beta < 1$ (bottom). Note that for λ small, the SIC range is r as the dominant constraint is that interfering nodes have smaller signal strengths, while for λ large, the SIC range is $\sqrt{K/(\pi\lambda)}$ as the dominant constraint is the bound, K, on the number of cancelable nodes. The function $\sqrt{K/(\pi\lambda)}$ is sketched as linear decreasing in λ for simplicity of exposition.

and the upper bound on TC is

$$c_{\text{ub}}^{\text{pSIC}}(\epsilon) = \frac{(-\log(1-\epsilon)+K)(1-\epsilon)}{\pi\beta^{\frac{2}{\alpha}}r^2}. \tag{22}$$

Proof: Looking at Fig. 3, the near field for $\beta > 1$ is

$$F_n^{\text{pSIC}} = \begin{cases} a\left(o, r, \beta^{\frac{1}{\alpha}}r\right), & \lambda < \frac{K}{\pi r^2} \\ a\left(o, \sqrt{\frac{K}{\pi\lambda}}, \beta^{\frac{1}{\alpha}}r\right), & \text{else} \end{cases} \tag{23}$$

for all λ, with associated area

$$\nu(F_n^{\text{pSIC}}) = \begin{cases} \pi r^2\left(\beta^{\frac{2}{\alpha}}-1\right), & \lambda < \frac{K}{\pi r^2} \\ \pi\left(\beta^{\frac{2}{\alpha}}r^2 - \frac{K}{\pi\lambda}\right), & \text{else.} \end{cases}. \tag{24}$$

The near field for $\beta \leq 1$ is

$$F_n^{\text{pSIC}} = \begin{cases} \emptyset, & \lambda < \frac{K}{\pi\beta^{\frac{2}{\alpha}}r^2} \\ a\left(o, \sqrt{\frac{K}{\pi\lambda}}, \beta^{\frac{1}{\alpha}}r\right), & \text{else} \end{cases} \tag{25}$$

with associated area

$$\nu(F_n^{\text{pSIC}}) = \begin{cases} 0, & \lambda < \frac{K}{\pi\beta^{\frac{2}{\alpha}}r^2} \\ \pi\left(\beta^{\frac{2}{\alpha}}r^2 - \frac{K}{\pi\lambda}\right), & \text{else.} \end{cases} \tag{26}$$

The outage probability and TC bounds given in the lemma are immediate from these expressions. □

The following lemma identifies the far-field region for all the cases indicated in Fig. 3, and gives the corresponding selection of s, t, u for Theorem 2.

Lemma 4: Consider perfect SIC. The far field for $\beta > 1$ is $F_f^{\text{pSIC}} = a(o, \beta^{\frac{1}{\alpha}}r, \infty)$ which corresponds to setting $s = t = u = \beta^{\frac{1}{\alpha}}r$ in Theorem 2. The far field for $\beta \leq 1$ is

$$F_f^{\text{pSIC}} = \begin{cases} a(o, r, \infty), & \lambda < \frac{K}{\pi r^2} \\ a\left(o, \sqrt{\frac{K}{\pi\lambda}}, \infty\right), & \frac{K}{\pi r^2} \leq \lambda < \frac{K}{\pi\beta^{\frac{2}{\alpha}}r^2} \\ a(o, \beta^{\frac{1}{\alpha}}r, \infty), & \text{else} \end{cases} \tag{27}$$

which corresponds to setting

$$s = t = u = \begin{cases} r, & \lambda < \frac{K}{\pi r^2} \\ \sqrt{\frac{K}{\pi\lambda}}, & \frac{K}{\pi r^2} \leq \lambda < \frac{K}{\pi\beta^{\frac{2}{\alpha}}r^2} \\ \beta^{\frac{1}{\alpha}}r, & \text{else} \end{cases} \tag{28}$$

in Theorem 2. The upper bound on outage probability with perfect SIC (pSIC) is

$$p_{\text{ub}}^{\text{pSIC}}(\lambda) = 1 - \left(1 - \exp\left\{-\Lambda^*\left(F_f^{\text{pSIC}}\right)\right\}\right) \times \exp\left\{-\lambda\nu\left(F_n^{\text{pSIC}}\right)\right\}. \tag{29}$$

The corresponding lower bound on the TC is obtained by solving $p_{\text{ub}}^{\text{pSIC}}(\lambda) = \epsilon$ for λ.

Proof: Recall that $F_n \cup F_f \cup b(o,1) = \mathbb{R}^2$, i.e., the near- and far-field partition the plane, excluding the automatically canceled region $b(o,1)$. With this in mind it is straightforward to identify the far field as the complement of the near field in Fig. 3. It is then simply a matter of selecting the parameters s, t, u in Theorem 2 to match the far field. For example, for $\beta > 1$, the far field is the region $a(o, \beta^{\frac{1}{\alpha}}r, \infty)$. Nodes in this region are not subject to cancellation, and as such the appropriate selection is $s = t = u = \beta^{\frac{1}{\alpha}}r$. □

Discussion: In Lemma 3, the TC upper bounds are the same for the cases of $\beta > 1$ and $\beta \leq 1$ except when the network density is low relative to the transmission range and number of cancelable users, i.e., $\lambda < \frac{K}{\pi r^2}$. Why?

When the network density is relatively low, the *received power constraint* dominates the performance; in other words, no matter how many nodes between $(1, r)$ are canceled, the uncancellable nodes that are farther than the desired transmitter dominate the outage probability. Therefore, this case is independent of K. In the case of a high-SIR requirement, any node in $a(o, 1, \beta^{\frac{1}{\alpha}}r)$

causes an outage, whereas with a relaxed SIR requirement no outage can occur from a single node in the near field.

On the other hand, when the network density is high, the *processing constraint* on the number of cancelable interferers dominates the performance. Due to complexity or latency constraints, only K interferers can be canceled, although more than K nodes are likely to be in $a(o,1,r)$ and thus cancelable. As can be seen in Fig. 3, the effective area of the near field decreases linearly with K, this causes the TC upper bound to increase additively with K. Note, however, that if K becomes sufficiently large, the outage probability lower bound can switch back into the regime that is independent of K. On the other hand, as long as λ is increased at the same rate as K, TC can increase linearly with K without limit in the perfect interference cancellation scenario as long as $\beta < 1$.

These dependencies will be further explored and quantified in the numerical and simulation results section along with the lower bounds on TC for pSIC.

VI. Imperfect Successive Interference Cancellation

The imperfect SIC model is a generalization of the pSIC model to capture the fact that not all interference power is removed under cancellation. The parameter $z \in (0,1)$ gives the *residual* interference for a canceled node, so that the interference is reduced by a factor of $1-z$. Although each interferer may be subject to a slightly different average cancellation error depending on its distance from the receiver, this model is adopted for simplicity in order to concretely consider the affect of varying levels of cancellation error.

Under imperfect SIC there are three regions:

- *perfect cancellation* within $b(o,1)$;
- *imperfect cancellation* within $a(o,1,\sqrt{\frac{K}{\pi\lambda}}\wedge r)$ by a factor $z \in (0,1)$;
- *no cancellation* in $a(o,\sqrt{\frac{K}{\pi\lambda}}\wedge r,\infty)$.

We define the cancellation region to be

$$C = a\left(o,1,\sqrt{\frac{K}{\pi\lambda}}\wedge r\right) \tag{30}$$

and the uncanceled region to be

$$E = a\left(o,\sqrt{\frac{K}{\pi\lambda}}\wedge r,\infty\right). \tag{31}$$

Note that $C\cap E=\emptyset$. It is possible under imperfect SIC for the near field to consist of both partially canceled as well as uncanceled locations

$$F_n = \{x\in\mathbb{R}^2 : z|x|^{-\alpha}\mathbf{1}_{x\in C} + |x|^{-\alpha}\mathbf{1}_{x\in E} > \beta\}. \tag{32}$$

Similarly, the near- and far-field interference may consist of contributions from both partially canceled and uncanceled nodes

$$\begin{aligned} Y_n &= z\sum_{i\in\Phi\cap F_n\cap C}|X_i|^{-\alpha} + \sum_{i\in\Phi\cap F_n\cap E}|X_i|^{-\alpha}\\ Y_f &= z\sum_{i\in\Phi\cap F_f\cap C}|X_i|^{-\alpha} + \sum_{i\in\Phi\cap F_f\cap E}|X_i|^{-\alpha}. \end{aligned} \tag{33}$$

As $z\in[0,1]$, there are three possible arrangements for $z\beta$, β, and 1: i) $1\le z\beta\le\beta$, ii) $z\beta\le 1\le\beta$, or iii) $z\beta\le\beta\le 1$. See Fig. 4. The figure is similar to Fig. 3 in that the shaded regions denote the near field as a function of the transmission density λ. The light shaded region is the near field lying outside of the cancellation region, and the dark shaded region is the near-field region lying inside the cancellation region. In particular, under imperfect cancellation, a single interfering node can be partially canceled *but is still capable causing an outage*. In several cases shown in the figure, the near field consists of an inner partially canceled annulus, and an outer uncanceled annulus. This observation is the motivation behind the particular parameterization used in Theorem 2.

Since an understanding of Fig. 4 is a prerequisite to understanding the subsequent lemmas, we briefly describe the regions in each of the three cases. First, the case $1\le z\beta\le\beta$ can be interpreted as the worst case in terms of outage, since either z is large (poor cancellation efficiency) or β is large (high required SIR). In fact, in this case interference cancellation does not improve the lower bound on outage probability, since even a single partially canceled node still has sufficient power to cause an outage because $(z\beta)^{\frac{1}{\alpha}}r > r$, i.e., the needed separation (even with some interference cancellation) is greater than the communication range. In the middle graph, $z\beta\le 1$, so this more accurate interference cancellation improves the lower bound for users farther away than $(z\beta)^{\frac{1}{\alpha}}r$; this is the unshaded wedge in this graph, which may be quite large as $z\to 0$. The bottom graph benefits both from interference cancellation in the range $[(z\beta)^{\frac{1}{\alpha}}r,\beta^{\frac{1}{\alpha}}r)$ and from a lax SIR requirement in the range $[\beta^{\frac{1}{\alpha}}r,\infty)$.

The following Lemma gives the lower bound on outage probability and corresponding upper bound on the TC by applying Theorem 1 to each of the near fields shown in Fig. 4; the proof is immediate from the figure.

Lemma 5: Consider imperfect SIC. For $1\le z\beta\le\beta$, the lower bound on the outage probability is

$$p_{\rm lb}^{\rm iSIC}(\lambda) = 1-\exp\left\{-\lambda\pi\left(\beta^{\frac{2}{\alpha}}r^2-1\right)\right\} \tag{34}$$

and the upper bound on TC is

$$c_{\rm lb}^{\rm iSIC}(\epsilon) = \frac{-(1-\epsilon)\log(1-\epsilon)}{\pi\left(\beta^{\frac{2}{\alpha}}r^2-1\right)}. \tag{35}$$

For $z\beta\le 1\le\beta$, the lower bound on the outage probability is shown in (36) at the top of the following page, and the upper bound on TC is

$$c_{\rm ub}^{\rm iSIC}(\epsilon) = \begin{cases} \frac{-(1-\epsilon)\log(1-\epsilon)}{\pi(r^2\left(\beta^{\frac{2}{\alpha}}\left(z^{\frac{2}{\alpha}}+1\right)-1\right)-1)}, & \lambda < \frac{K}{\pi r^2}\\ \frac{(1-\epsilon)(-\log(1-\epsilon)+K)}{\pi\left(\beta^{\frac{2}{\alpha}}r^2 l\left(z^{\frac{2}{\alpha}}+1\right)-1\right)}, & \frac{K}{\pi r^2}\le\lambda<\frac{K}{\pi(z\beta)^{\frac{2}{\alpha}}r^2}\\ \frac{-(1-\epsilon)\log(1-\epsilon)}{\pi\left(\beta^{\frac{2}{\alpha}}r^2-1\right)}, & \text{else.}\end{cases} \tag{37}$$

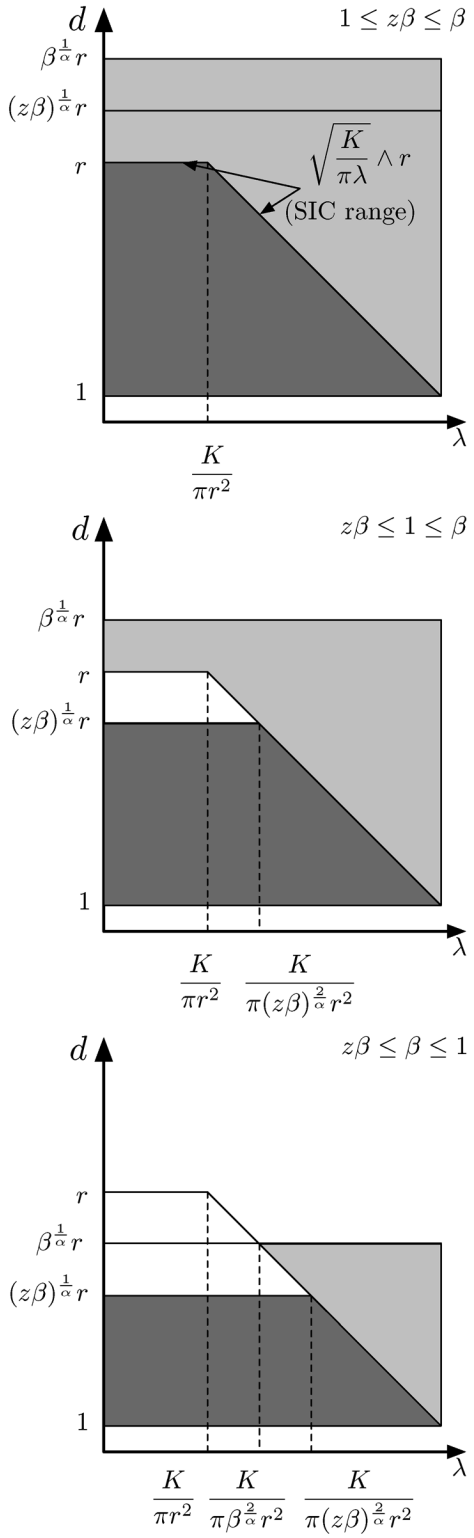

Fig. 4. Illustration of the near-field region (shaded) for the imperfect cancellation model. The x-axis is the spatial density of attempted transmissions (λ) and the y-axis is the distance from the origin d. The light shaded region is the near field lying outside of the cancellation region, while the dark shaded region is the near field lying inside the cancellation region. The shape of the near field depends upon whether $1 \le z\beta \le \beta$ (top), $z\beta \le 1 \le \beta$ (middle), or $z\beta \le \beta \le 1$ (bottom). Note that for λ small, the SIC range is r as the dominant constraint is that interfering nodes have smaller signal strengths, while for λ large, the SIC range is $\sqrt{K/(\pi\lambda)}$ as the dominant constraint is the bound, K, on the number of cancelable nodes. The function $\sqrt{K/(\pi\lambda)}$ is sketched as linear decreasing in λ for simplicity of exposition.

For $z\beta \le \beta \le 1$, the lower bound on the outage probability is shown in (38), also at the top of the following page, and the upper bound on TC is

$$c_{\rm ub}^{\rm iSIC}(\epsilon) = \begin{cases} \frac{-(1-\epsilon)\log(1-\epsilon)}{\pi\left((z\beta)^{\frac{2}{\alpha}} r^2 - 1\right)}, & \lambda < \frac{K}{\pi\beta^{\frac{2}{\alpha}} r^2} \\ \frac{(1-\epsilon)(-\log(1-\epsilon)+K)}{\pi\left(\beta^{\frac{2}{\alpha}} r^2 \left(z^{\frac{2}{\alpha}}+1\right)-1\right)}, & \frac{K}{\pi\beta^{\frac{2}{\alpha}} r^2} \le \lambda < \frac{K}{\pi(z\beta)^{\frac{2}{\alpha}} r^2} \\ \frac{-(1-\epsilon)\log(1-\epsilon)}{\pi\left(\beta^{\frac{2}{\alpha}} r^2 - 1\right)}, & \text{else.} \end{cases} \tag{39}$$

Proof: The near field for $1 \le z\beta \le \beta$ consists of

$$F_n^{\rm iSIC} = a\left(o, 1, \beta^{\frac{1}{\alpha}} r\right) \tag{40}$$

with associated area

$$\nu\left(F_n^{\rm iSIC}\right) = \pi\left(\beta^{\frac{2}{\alpha}} r^2 - 1\right). \tag{41}$$

The near field for $z\beta \le 1 \le \beta$ is shown in (42) at the top of the following page,with associated area shown in (43), also at the top of the following page. The near field for $z\beta \le \beta \le 1$ is shown in (44) at the top of the following page, with associated area as in (45), at the top of the following page.

The outage probability and TC bounds given in the lemma are immediate from these expressions. □

Lemma 6: Consider imperfect SIC. The far field for $1 \le z\beta \le \beta$ is $F_f^{\rm iSIC} = a(o, \beta^{\frac{1}{\alpha}} r, \infty)$ which corresponds to setting $s = t = u = \beta^{\frac{1}{\alpha}} r$ in Theorem 2. The far field for $z\beta \le 1 \le \beta$ is given in (46) at the bottom of the following page, which corresponds to setting

$$\begin{aligned} &s = (z\beta)^{\frac{1}{\alpha}} r, t = r, u = \beta^{\frac{1}{\alpha}} r, && \lambda < \tfrac{K}{\pi r^2} \\ &s = (z\beta)^{\frac{1}{\alpha}} r, t = \sqrt{\tfrac{K}{\pi\lambda}}, u = \beta^{\frac{1}{\alpha}} r, && \tfrac{K}{\pi r^2} \le \lambda < \tfrac{K}{\pi\beta^{\frac{2}{\alpha}} r^2} \\ &s = t = u = \beta^{\frac{1}{\alpha}} r, && \text{else} \end{aligned} \tag{47}$$

in Theorem 2. The far field for $z\beta \le \beta \le 1$ is as shown in (48) at the top of the subsequent page, which corresponds to setting, shown in (49), also at the top of the subsequent page, in Theorem 2. The upper bound on outage probability with imperfect SIC is

$$\begin{aligned} p_{\rm ub}^{\rm iSIC}(\lambda) = 1 - \left(1 - \exp\left\{-\Lambda^*\left(F_f^{\rm iSIC}\right)\right\}\right) \\ \times \exp\left\{-\lambda\nu\left(F_n^{\rm iSIC}\right)\right\}. \end{aligned} \tag{50}$$

The corresponding lower bound on the TC is obtained by solving $p_{\rm ub}^{\rm iSIC}(\lambda) = \epsilon$ for λ.

Proof: The far field for the imperfect SIC model may be identified from Fig. 4, just as was done for the perfect SIC model using Fig. 3. □

Discussion: In Lemma 5, seven different TC upper bounds were given for the different relative values of $z\beta, \beta$, and 1, and also depending on the network density λ in relation to other parameters. These seven bounds can be grouped into three

$$p_{\mathrm{lb}}^{\mathrm{iSIC}}(\lambda) = \begin{cases} 1-\mathrm{e}^{-\lambda\pi\left(r^2\left(\beta^{\frac{2}{\alpha}}\left(z^{\frac{2}{\alpha}}+1\right)-1\right)-1\right)}, & \lambda < \frac{K}{\pi r^2} \\ 1-\mathrm{e}^{-\lambda\pi\left(\beta^{\frac{2}{\alpha}} r^2\left(z^{\frac{2}{\alpha}}+1\right)-1\right)+K}, & \frac{K}{\pi r^2} \le \lambda < \frac{K}{\pi (z\beta)^{\frac{2}{\alpha}} r^2} \\ 1-\mathrm{e}^{-\lambda\pi\left(\beta^{\frac{2}{\alpha}} r^2-1\right)}, & \text{else} \end{cases} \tag{36}$$

$$p_{\mathrm{lb}}^{\mathrm{iSIC}}(\lambda) = \begin{cases} 1-\mathrm{e}^{-\lambda\pi((z\beta)^{\frac{2}{\alpha}} r^2-1)}, & \lambda < \frac{K}{\pi\beta^{\frac{2}{\alpha}} r^2} \\ 1-\mathrm{e}^{-\lambda\pi(\beta^{\frac{2}{\alpha}} r^2(z^{\frac{2}{\alpha}}+1)-1)+K}, & \frac{K}{\pi\beta^{\frac{2}{\alpha}} r^2} \le \lambda < \frac{K}{\pi (z\beta)^{\frac{2}{\alpha}} r^2}, \\ 1-\mathrm{e}^{-\lambda\pi(\beta^{\frac{2}{\alpha}} r^2-1)}, & \text{else} \end{cases} \tag{38}$$

$$F_n^{\mathrm{iSIC}} = \begin{cases} a(o,1,(z\beta)^{\frac{1}{\alpha}} r) \cup a\left(o,r,\beta^{\frac{1}{\alpha}} r\right), & \lambda < \frac{K}{\pi r^2} \\ a\left(o,1,(z\beta)^{\frac{1}{\alpha}} r\right) \cup a\left(o,\sqrt{\frac{K}{\pi\lambda}},\beta^{\frac{1}{\alpha}} r\right), & \frac{K}{\pi r^2} \le \lambda < \frac{K}{\pi (z\beta)^{\frac{2}{\alpha}} r^2} \\ a\left(o,1,\beta^{\frac{1}{\alpha}} r\right), & \text{else} \end{cases} \tag{42}$$

$$\nu(F_n^{\mathrm{iSIC}}) = \begin{cases} \pi\left(r^2\left(\beta^{\frac{2}{\alpha}}\left(z^{\frac{2}{\alpha}}+1\right)-1\right)-1\right), & \lambda < \frac{K}{\pi r^2} \\ \pi\left(\beta^{\frac{2}{\alpha}} r^2 (z^{\frac{2}{\alpha}}+1)-1\right) - \frac{K}{\lambda}, & \frac{K}{\pi r^2} \le \lambda < \frac{K}{\pi (z\beta)^{\frac{2}{\alpha}} r^2} \\ \pi\left(\beta^{\frac{2}{\alpha}} r^2-1\right), & \text{else.} \end{cases} \tag{43}$$

$$F_n^{\mathrm{iSIC}} = \begin{cases} a\left(o,1,(z\beta)^{\frac{1}{\alpha}} r\right), & \lambda < \frac{K}{\pi\beta^{\frac{2}{\alpha}} r^2} \\ a\left(o,1,(z\beta)^{\frac{1}{\alpha}} r\right) \cup a\left(o,\sqrt{\frac{K}{\pi\lambda}},\beta^{\frac{1}{\alpha}} r\right), & \frac{K}{\pi\beta^{\frac{2}{\alpha}} r^2} \le \lambda < \frac{K}{\pi (z\beta)^{\frac{2}{\alpha}} r^2} \\ a\left(o,1,\beta^{\frac{1}{\alpha}} r\right), & \text{else} \end{cases} \tag{44}$$

$$\nu(F_n^{\mathrm{iSIC}}) = \begin{cases} \pi\left((z\beta)^{\frac{2}{\alpha}} r^2-1\right), & \lambda < \frac{K}{\pi\beta^{\frac{2}{\alpha}} r^2} \\ \pi\left(\beta^{\frac{2}{\alpha}} r^2\left(z^{\frac{2}{\alpha}}+1\right)-1\right) - \frac{K}{\lambda}, & \frac{K}{\pi\beta^{\frac{2}{\alpha}} r^2} \le \lambda < \frac{K}{\pi (z\beta)^{\frac{2}{\alpha}} r^2} \\ \pi\left(\beta^{\frac{2}{\alpha}} r^2-1\right), & \text{else.} \end{cases} \tag{45}$$

different classes as follows, for better comprehension of their meaning.

1) No explicit dependence on z or K. Three of these upper bounds exist and are identical: for $1 \le z\beta \le \beta$, and for high λ in the other two cases. Here, interference cancellation has no measurable effect on the capacity upper bound due to a combination of poor cancellation accuracy (high z), high required SIR, low number of cancelable users K, and/or a high network density λ relative to the aforementioned parameters. Note that although the TC in this regime does not depend on the values of z or K, the regime itself is defined in part by z and K.
2) Dependence on z but not on K. This occurs twice, and is the case for low network density and reasonably accurate interference cancellation (low z). Intuitively, in this regime there are not enough interferers to cause the processing constraint

$$F_f^{\mathrm{iSIC}} = \begin{cases} a\left(o,(z\beta)^{\frac{1}{\alpha}} r,r\right) \cup a\left(o,\beta^{\frac{1}{\alpha}} r,\infty\right), & \lambda < \frac{K}{\pi r^2} \\ a\left(o,(z\beta)^{\frac{1}{\alpha}} r,\sqrt{\frac{K}{\pi\lambda}}\right) \cup a\left(o,\beta^{\frac{1}{\alpha}} r,\infty\right), & \frac{K}{\pi r^2} \le \lambda < \frac{K}{\pi (z\beta)^{\frac{2}{\alpha}} r^2} \\ a\left(o,\beta^{\frac{1}{\alpha}} r,\infty\right), & \text{else} \end{cases} \tag{46}$$

$$F_f^{\text{iSIC}} = \begin{cases} a\left(o,(z\beta)^{\frac{1}{\alpha}}r,r\right)\cup a(o,r,\infty), & \lambda < \frac{K}{\pi r^2} \\ a\left(o,(z\beta)^{\frac{1}{\alpha}}r,\sqrt{\frac{K}{\pi\lambda}}\right)\cup a\left(o,\sqrt{\frac{K}{\pi\lambda}},\infty\right), & \frac{K}{\pi r^2} \le \lambda < \frac{K}{\pi\beta^{\frac{2}{\alpha}}r^2} \\ a\left(o,(z\beta)^{\frac{1}{\alpha}}r,\sqrt{\frac{K}{\pi\lambda}}\right)\cup a(o,\beta^{\frac{1}{\alpha}}r,\infty), & \frac{K}{\pi\beta^{\frac{2}{\alpha}}r^2} \le \lambda < \frac{K}{\pi(z\beta)^{\frac{2}{\alpha}}r^2} \\ a\left(o,\beta^{\frac{1}{\alpha}}r,\infty\right), & \text{else} \end{cases}, \tag{48}$$

$$\begin{cases} s=(z\beta)^{\frac{1}{\alpha}}r, t=u=r, & \lambda < \frac{K}{\pi r^2} \\ s=(z\beta)^{\frac{1}{\alpha}}r, t=u=\sqrt{\frac{K}{\pi\lambda}}, & \frac{K}{\pi r^2} \le \lambda < \frac{K}{\pi\beta^{\frac{2}{\alpha}}r^2} \\ s=(z\beta)^{\frac{1}{\alpha}}r, t=\sqrt{\frac{K}{\pi\lambda}}, u=\beta^{\frac{1}{\alpha}}r, & \frac{K}{\pi\beta^{\frac{2}{\alpha}}r^2} \le \lambda < \frac{K}{\pi(z\beta)^{\frac{2}{\alpha}}r^2} \\ s=t=u=\beta^{\frac{1}{\alpha}}r, & \text{else} \end{cases} \tag{49}$$

to become an issue. The capacity upper bound does increase as the cancellation accuracy improves, however.

3) Dependence on both z and K. This also occurs twice, in a moderate density regime where cancellation helps (i.e., z is sufficiently small), and the more users that can be canceled the better. Once the network density increases, there is likely to be a strong user that cannot be sufficiently canceled due to high z or low K, so we are back to scenario 1), above.

These dependencies will be further explored and quantified in the next section along with the lower bounds on TC, which are not available in closed form so not discussed here.

VII. Numerical and Simulation Results

All numerical results are computed using Mathematica; all simulation results are obtained from a Perl program written by the authors. Simulations are run until a 95% confidence intervals with relative error of at most 5% is achieved. In all cases, the error bars denoting the confidence interval are no wider than the symbol used to indicate the location of the point estimator, and are therefore not shown.

It is important to note that the simulation results are for *the actual SIC system*, not the approximate system. In particular, the simulated (K,z) SIC receiver cancels up to the first K interferers within radius r by a factor of $1-z$ (as opposed to the approximate system that cancels *all* nodes in $a(o,1,\sqrt{K/(\pi\lambda)}\wedge r)$ by $1-z$). The simulation results for the approximate system all lie between the given bounds and are not shown. The simulation results that are shown *do not in all cases lie between the bounds*: this is because the numerical bounds hold for the *approximate* SIC model, not the *actual* SIC model. The numerical results will illustrate when the approximate SIC model is good and when it fails to capture the performance of the actual SIC model.

All simulation results include ambient (thermal) noise corresponding to a signal-to-noise ratio (SNR) of 100 (20 dB), i.e.,

$$\text{SNR} = \frac{\rho r^{-\alpha}}{\sigma^2} = 100 \Rightarrow \sigma^2 = \frac{\rho}{100 r^{\alpha}}. \tag{51}$$

For the default values of $\rho = 1$ W, $r = 10$ m, and $\alpha = 4$ we obtain a noise power of $\sigma^2 = 10^{-6}$ W. Both ρ and σ^2 should technically be attenuated by the measured path loss at $d_o = 1$ m, a quantity that is close to $\frac{c}{4\pi f_c}$, where c is the speed of light and f_c is the carrier frequency. Neglecting this effect does not change the SNR. The noise has a negligible impact on the simulation results.

Here and throughout this section we consider two fundamentally different scenarios: a small SIR requirement ($\beta = 1/10 < 1$) and a large SIR requirement ($\beta = 10 > 1$). We will often speak of the small SIR requirement scenario as the *spreading* case, since spreading reduces the SIR requirement by a factor of M. If the nominal SIR requirement is 10 then we obtain $\beta = 1/10$ by spreading with $M = 100$. A prominent theme throughout our discussion will be that SIC and spreading work well together, and that SIC without spreading may be ineffective.

Unless stated otherwise, all results employ a path loss attenuation constant of $\alpha = 4$ and a transmission distance of $r = 10$ m. The notation UB and LB denotes the upper and lower bound on the corresponding y-axis quantity. For clarity of presentation, simulation results are shown for only a subset of the plots.

Fig. 5 contains five plots of the TC, $c(\epsilon)$, versus ϵ and one plot of the outage probability, $p(\lambda)$, versus λ (top left). The top row shows results for the no SIC model, the middle row shows results for the perfect SIC model, and the bottom row shows results for the imperfect SIC model.

The **top row** in Fig. 5 gives $p(\lambda)$ and $c(\epsilon)$ for the no SIC case for both $\beta = 1/10$ and $\beta = 10$. The bounds are seen to be reasonably tight for both $p(\lambda)$ and $c(\epsilon)$. Moreover, the impact of spreading (reducing β) is apparent: for small λ, the outage probability is decreased by an order of magnitude, and $c(\epsilon)$ is increased by the same factor. The simulation results lie between the bounds.

The **middle row** in Fig. 5 gives results for the perfect SIC case. The left graph shows the TC bounds and simulation results for $K = 1$ and $\beta = 1/10, 10$, while the right shows the TC for $K = 10$ and $\beta = 1/10, 10$. Note that the approximate SIC model captures the behavior of the actual (simulated) SIC model for all cases except when $\beta = 1/10$ and $K = 1$. Thus, the approximate SIC model is a poor model for perfect SIC and small K. There are two contributions to this performance discrepancy. First, recall from Fig. 3 that there is no reliable lower bound event for $\beta < 1$ and λ small. Second, in perfect SIC with $K = 1$, the actual SIC model cancels *the sole dominant interferer* in $a(o,1,r)$ (if there is one), while the approximate model cancels *all* nodes in $a(o,1,r)$ (for λ small). This approximation

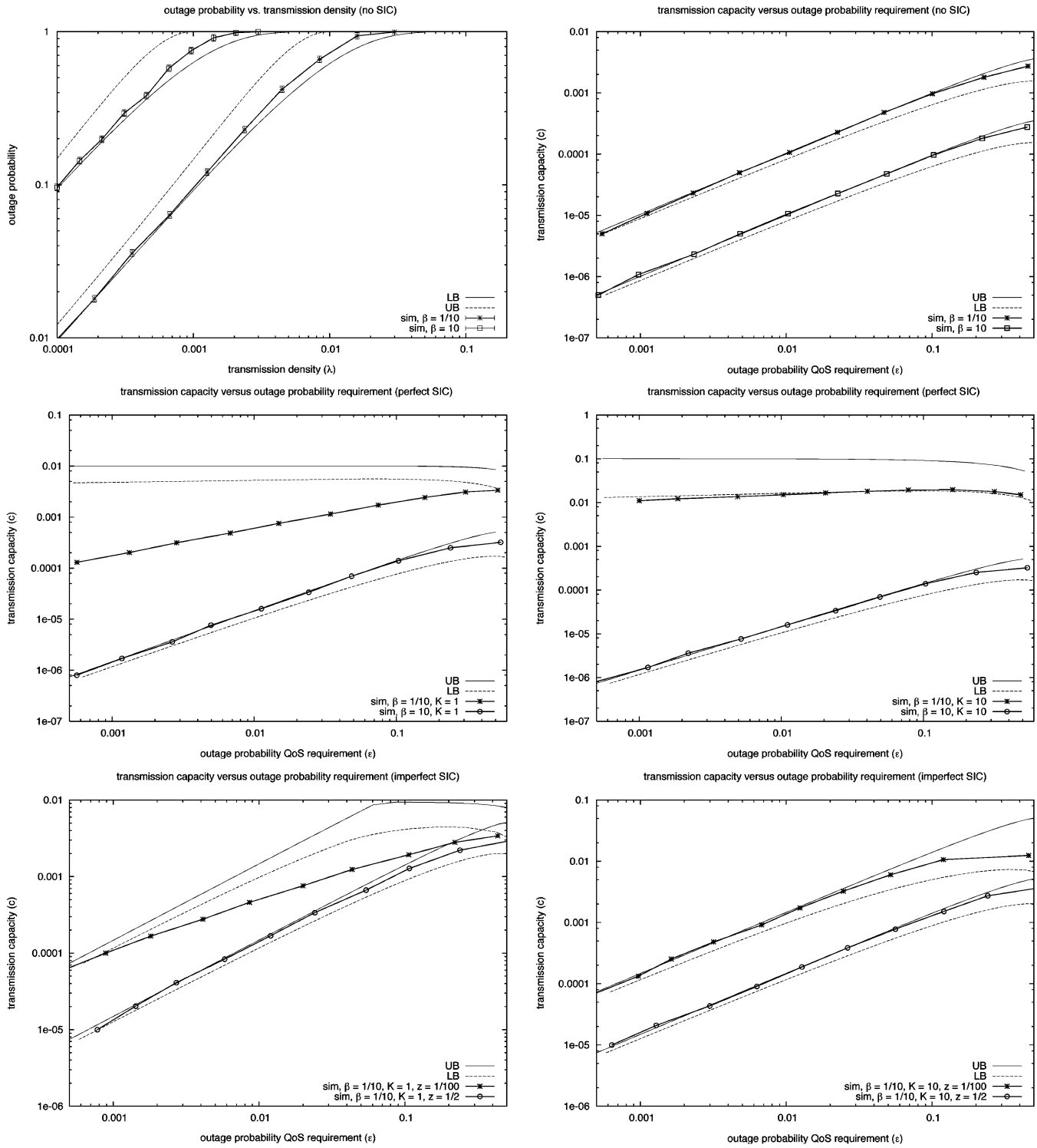

Fig. 5. Outage probability $p(\lambda)$ versus λ (top left), and TC $c(\epsilon)$ versus ϵ (all other plots). The top row gives results for no SIC, the middle row for perfect SIC, the bottom row for imperfect SIC.

is clearly rather poor in the regime where there is on average more than one node in $a(o,1,r)$.

Comparing the perfect SIC results for $\beta = 10$ and $K = 1, 10$ with the nSIC results for $\beta = 10$ we see all three plots coincide. This is because, as shown in Fig. 3, the lower bound on outage probability is independent of K for $\beta > 1$. This is the first result supporting the claim that SIC should be coupled with spreading. In particular, using SIC without spreading means the SIR requirement may be high enough such that the dominant SIC constraint is the power constraint, rather than the bound on the number of cancelable nodes (K). More concretely, the problem with SIC when $\beta > 1$ is that the SIC region covers only a (possibly negligibly) small portion of the near field (which dominates $p(\lambda)$). For $\beta > 1$, the near field has area approx-

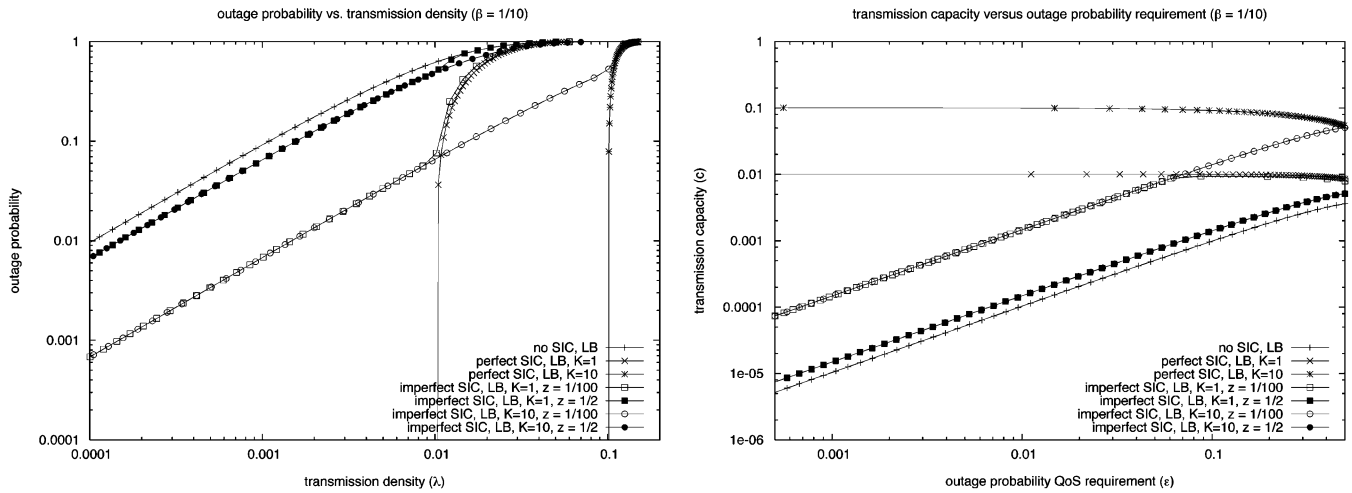

Fig. 6. **Left**: outage probability, $p(\lambda)$, versus transmission density, λ. **Right:** TC, $c(\epsilon)$, versus the QoS requirement ϵ. Both plots are for $\beta = 1/10$.

imately $\pi\beta^{\frac{2}{\alpha}}r^2$ while the cancellation region has areas πr^2. Thus, the fraction of the near field covered by cancellation is $\beta^{-\frac{2}{\alpha}}$; in the case of $\beta = 10$ and $\alpha = 4$ this is $1/\sqrt{10} \approx 1/3$, i.e., only one third of the near-field region is addressed by cancellation, regardless of K.

The **bottom row** of Fig. 5 gives results for the imperfect SIC case. The left graph shows the TC bounds and simulation results for $\beta = 1/10, K = 1$, and $z = 1/100, 1/2$, while the right graph shows the TC for $\beta = 1/10, K = 10$, and $z = 1/100, 1/2$. The bounds are accurate for all three cases except for $K = 1$ and $z = 1/100$. This is natural given the discussion of the perfect SIC case with $K = 1$ above since $z = 1/100$ is very close to perfect SIC of $z = 0$. The most significant point to note is the large sensitivity to z for small ϵ and $\beta = 1/10$ and $K = 10$. In particular, at $\epsilon = 0.001$ the TC for perfect SIC, $\beta = 1/10, K = 10$ is roughly 100 times that of imperfect SIC with $z = 1/100$, which is in turn roughly 10 times the TC with $z = 1/2$. On the other hand, looking at the case $\beta = 1/10$ and $K = 1$, we see the TC under imperfect SIC with $z = 1/100$ is very close to that of perfect SIC.

Not shown are imperfect SIC results for $\beta = 10$. These are very similar to the results for perfect SIC and no SIC for $\beta = 10$; in the high-β regime, the TC is relatively insensitive to cancellation (both K and z).

Fig. 6 contains two plots showing the lower bound on $p(\lambda)$ versus λ (on the left), and the upper bound on $c(\epsilon)$ versus ϵ (on the right), all for the case of $\beta = 1/10$. As expected, the perfect SIC curve always has a lower $p(\lambda)$ than the imperfect SIC case (for all z and fixed K), which in turn always has a lower $p(\lambda)$ than the no SIC case. Similarly, $c(\epsilon)$ for perfect SIC is always higher than $c(\epsilon)$ for imperfect SIC (for all z and fixed K), which in turn is always higher than the no SIC case. The results highlight that for $\beta = 1/10$ there is great sensitivity to z but small sensitivity to K. At $z = 1/2$, there is no appreciable reduction in $p(\lambda)$ or increase in $c(\epsilon)$ (compared with the nSIC case), but at $z = 1/100$ the increase and decrease is about a factor of 10.

Not shown are the corresponding results for the case when $\beta = 10$. Due to the limited dependence on z, K, there is almost no distinction between the lower bounds on $p(\lambda)$ for no SIC and the lower bounds on $p(\lambda)$ for perfect SIC. The same is true for the upper bound on $c(\epsilon)$. As shown in Fig. 4, the near field for imperfect SIC when $1 \leq z\beta \leq \beta$ is the same as the near field without SIC. It follows that there can be little impact of applying SIC when $\beta \gg 1$.

Fig. 7 contains four plots varying four other model parameters besides λ and ϵ. The **top left** graph shows the outage probability versus the path loss exponent $\alpha > 2$. Shown are lower and upper bounds for both nSIC and imperfect SIC with $K = 10, z = 1/100$, and imperfect SIC with $K = 10, z = 1/10$. The bounds are seen to be reasonably tight, and the tightness improves as α increases. This is attributable to the fact that for large α, the outage probability is dominated by near-field interferers, so that the looseness of the Chernoff bound on the far field $p(\lambda)$ has a negligible impact.

The **top right** graph shows the upper bounds on the TC (for $\epsilon = 0.1$) versus the transmission radius r, for nSIC, pSIC ($K = 10$), and imperfect SIC ($K = 10, z = 1/100$ and $K = 1z = 1/100$). Spreading is assumed, so that $\beta = 1/10$. As expected the TC for nSIC is at the bottom. Note the dramatic increase in $c(\epsilon)$ obtained by adding a single cancelable node ($K = 1$), and the additional dramatic increase in $c(\epsilon)$ obtained by increasing up to $K = 10$ cancelable nodes. Also interesting is that for $K = 1$ using $z = 1/100$ nets most of the increase in TC, while for $K = 10$, using $z = 1/100$ is effectively the same as using $K = 1$. This can be understood by appealing to the $z\beta \leq \beta \leq 1$ panel in Fig. 4. The lesson learned is that both K and z can have dramatic or negligible impacts on performance depending upon the the transmission density λ and the SIR requirement β.

The **bottom left** graph shows upper bounds on TC (for $\epsilon = 0.01$ and $\beta = 1/10$) for nSIC, pSIC, and imperfect SIC as z is logarithmically varied from 0 to 1. Of course the nSIC and pSIC $p(\lambda)$ are independent of z; the plot confirms the desired behavior that the imperfect SIC outage probability switches from pSIC ($z = 0$) to nSIC ($z = 1$). It is striking how fast TC is lost as z is increased. By $z = 0.01$ nearly two orders of magnitude are lost; this is very distinct from cellular systems with centralized power control, where even with $z = 0.5$ achieving about half the gain of pSIC is possible [26].

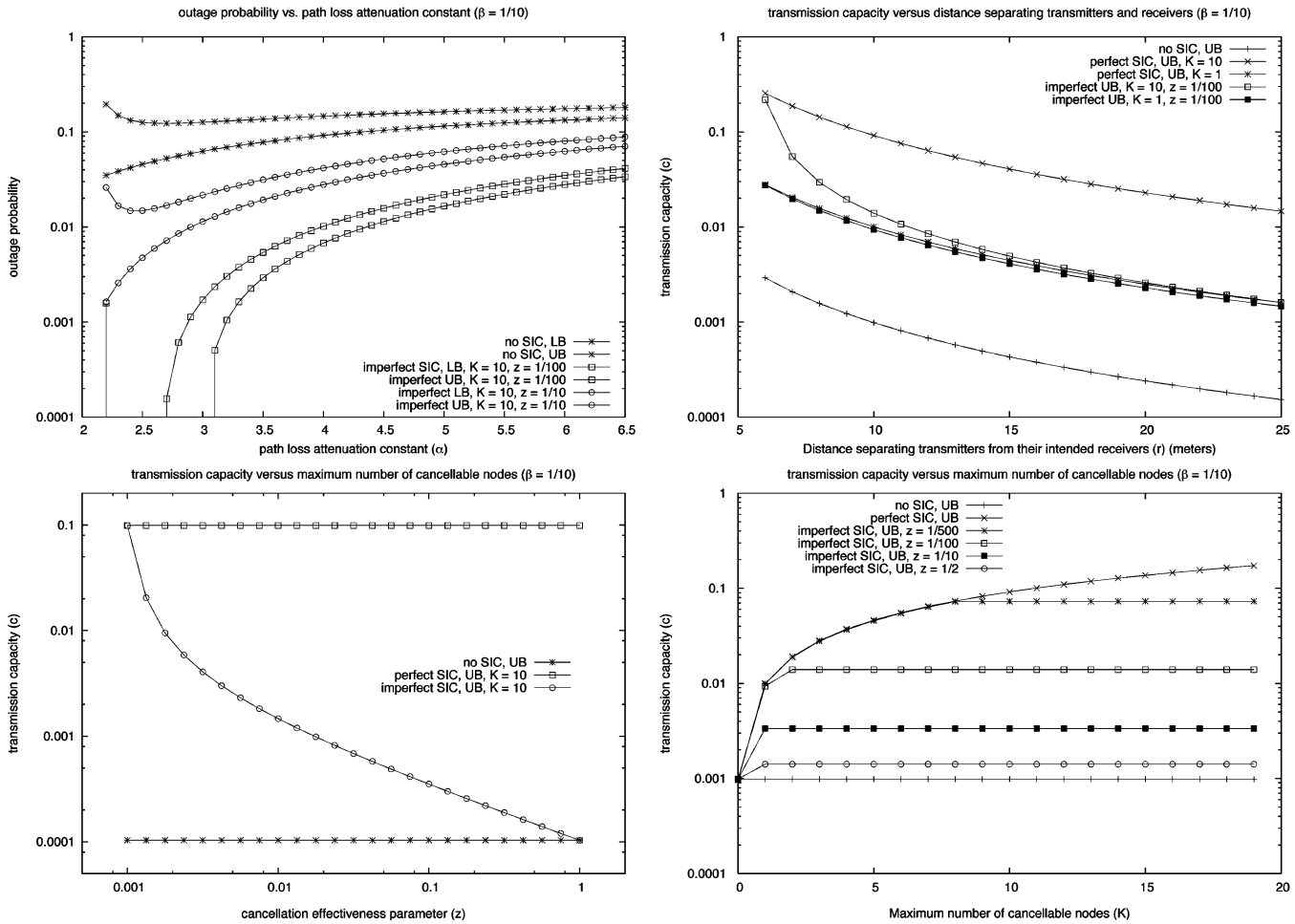

Fig. 7. **Top left**: outage probability versus the path loss exponent α. **Top right**: TC versus the transmission radius r. **Bottom left**: TC versus the cancellation effectiveness parameter z. **Bottom right**: TC versus the number of cancelable nodes K.

The **bottom right** graph shows $c(\epsilon)$ (for $\epsilon = 0.1$) versus the number of cancelable nodes, K. The no SIC $c(\epsilon)$ is the bottom curve, and of course is independent of K. The pSIC $c(\epsilon)$ is the upper curve. The imperfect SIC $c(\epsilon)$ is shown for $z = 1/500, 1/100, 1/10, 1/2$. Clearly, reducing z achieves a higher TC. What is interesting to note is that, confirming the discussion in the top right of Fig. 7, the region where z affects the $c(\epsilon)$ depends upon K. In particular, for K small, $c(\epsilon)$ is highly sensitive to z, while for K large, $c(\epsilon)$ is less sensitive. We also note that unless the cancellation is extremely accurate, i.e., $z < 0.01$, there is no appreciable gain to canceling more than one interferer. These results might be of interest to SIC hardware designers as they identify how reducing z or increasing K will or will not affect the performance of the transceiver.

VIII. Conclusion

The primary contribution of this work is a tractable framework for analyzing the performance improvement obtainable through the use of successive interference cancellation in wireless *ad hoc* networks. Through the use of stochastic geometric models and analysis we are able to obtain (in most cases) reasonably tight closed-form expressions for the TC in terms of the fundamental SIC parameters, i.e., the number of cancelable nodes K and the cancellation effectiveness z. Our analysis and simulation results support the claims that i) SIC is most effective when coupled with spreading to reduce the SINR requirement, and ii) performance is often highly sensitive to the cancellation effectiveness parameter but less sensitive to the number of cancelable nodes.

Appendix
Proof of Theorem 1

The proof runs as follows:

$$\begin{aligned} p(\lambda) &= \mathbb{P}^0\left(Y > \frac{1}{\beta r^\alpha}\right) \\ &> \mathbb{P}^0\left(Y_n > \frac{1}{\beta r^\alpha}\right) \\ &= 1 - \mathbb{P}^0(\Phi \cap F_n = \emptyset) \\ &= 1 - \exp\left\{-\lambda \nu(F_n)\right\}. \end{aligned} \tag{52}$$

The inequality follows from the fact that $Y = Y_n + Y_f$ implying $Y > Y_n$. The event $\{Y_n > \frac{1}{\beta r^\alpha}\}$ is the same as the event $\{\Phi \cap F_n \neq \emptyset\}$ (the event that there are one or more near field interferers) since the normalized interference contribution of any near-field node is at least $\frac{1}{\beta r^\alpha}$ by construction. The final equality is obtained by noting that the number of nodes of a Poisson field Φ lying in a bounded region $A \subset \mathbb{R}^2$ is a Poisson

random variable with parameter $\lambda\nu(A)$. In this case, the probability that there are no nodes in F_n is $\mathrm{e}^{-\lambda\nu(F_n)}$. □

Proof of Theorem 2

The following proof finds the moment generating function (MGF) of the far-field interference lying within the disk $b(o,v)$ for $v > u$, then finds the MGF for the entire plane by letting $v \to \infty$. This same technique is applied by Sousa and Silvester in [14] in a distinct but related context.

Let $N^v = |\Phi \cap b(o,v)| \sim \text{Poisson}(\lambda\pi v^2)$ be the number of nodes in $b(o,v)$, for $v \geq u$. Recall that the distribution of the distance from the origin of a node placed uniformly at random in $b(o,v)$ is

$$\mathbb{P}(|X| \leq x \big| |X| \leq v) = \left(\frac{x}{v}\right)^2, \qquad 0 \leq x \leq v. \tag{53}$$

The corresponding density is $\frac{2x}{v^2}$. The far-field interference seen at the origin is

$$Y_f^v = z\sum_{i=1}^{N^v} |X_i|^{-\alpha}\mathbf{1}_{s<|X_i|\leq t} + \sum_{i=1}^{N^v} |X_i|^{-\alpha}\mathbf{1}_{u<|X_i|\leq v}. \tag{54}$$

The MGF of the random variable Y_f^v is

$$\begin{aligned} M_{Y_f^v}(\theta) &= \mathbb{E}[(\mathbb{E}[\exp\{\theta z|X|^{-\alpha}\mathbf{1}_{s<|X|\leq t} \\ &\quad + \theta|X|^{-\alpha}\mathbf{1}_{u<|X|\leq v}\}])^{N^v}] \\ &= \mathbb{E}\left[\left(\int_0^s \frac{2x}{v^2}\mathrm{d}x + \int_s^t \mathrm{e}^{\theta z x^{-\alpha}}\frac{2x}{v^2}\mathrm{d}x \right.\right. \\ &\quad \left.\left. + \int_t^u \frac{2x}{v^2}\mathrm{d}x + \int_u^v \mathrm{e}^{\theta x^{-\alpha}}\frac{2x}{v^2}\mathrm{d}x\right)^{N^v}\right]. \end{aligned} \tag{55}$$

The expectation is with respect to the Poisson distribution of N^v; the resulting expression is simplified by using the series $\mathrm{e}^x = \sum_{k=0}^{\infty}\frac{x^k}{k!}$, as shown below.

$$\begin{aligned} M_{Y_f^v}(\theta) &= \sum_{k=0}^{\infty}\mathrm{e}^{-\pi\lambda v^2}\frac{(\pi\lambda v^2)^k}{k!}\left(\int_0^s \frac{2x}{v^2}\mathrm{d}x \right. \\ &\quad + \int_s^t \mathrm{e}^{\theta z x^{-\alpha}}\frac{2x}{v^2}\mathrm{d}x + \int_t^u \frac{2x}{v^2}\mathrm{d}x \\ &\quad \left. + \int_u^v \mathrm{e}^{\theta x^{-\alpha}}\frac{2x}{v^2}\mathrm{d}x\right)^k \\ &= \exp\left\{-\pi\lambda v^2 + \pi\lambda v^2\left(\int_0^s \frac{2x}{v^2}\mathrm{d}x \right.\right. \\ &\quad + \int_s^t \mathrm{e}^{\theta z x^{-\alpha}}\frac{2x}{v^2}\mathrm{d}x + \int_t^u \frac{2x}{v^2}\mathrm{d}x \\ &\quad \left.\left. + \int_u^v \mathrm{e}^{\theta x^{-\alpha}}\frac{2x}{v^2}\mathrm{d}x\right)\right\} \\ &= \exp\left\{2\pi\lambda\left(-\int_0^v x\mathrm{d}x + \int_0^s x\mathrm{d}x \right.\right. \\ &\quad + \int_s^t \mathrm{e}^{\theta z x^{-\alpha}}x\mathrm{d}x + \int_t^u x\mathrm{d}x \\ &\quad \left.\left. + \int_u^v \mathrm{e}^{\theta x^{-\alpha}}x\mathrm{d}x\right)\right\} \\ &= \exp\left\{2\pi\lambda\left(\int_s^t \left(\mathrm{e}^{\theta z x^{-\alpha}} - 1\right)x\mathrm{d}x \right.\right. \\ &\quad \left.\left. + \int_u^v \left(\mathrm{e}^{\theta x^{-\alpha}} - 1\right)x\mathrm{d}x\right)\right\}. \end{aligned} \tag{56}$$

Taking the limit as $v \to \infty$ yields

$$\begin{aligned} M_{Y_f}(\theta) = \exp\left\{2\pi\lambda\left[\int_s^t x\left(\mathrm{e}^{\theta z x^{-\alpha}} - 1\right)\mathrm{d}x \right.\right. \\ \left.\left. + \int_u^{\infty} x\left(\mathrm{e}^{\theta x^{-\alpha}} - 1\right)\mathrm{d}x\right]\right\}. \end{aligned} \tag{57}$$

The expression for the Chernoff bound is straightforward once the MGF is obtained: the rate function is the convex dual of the log MGF. □

Proof of Theorem 3

The proof is a simple conditioning argument on the two events $\{Y_n > y\}$ and $\{Y_n \leq y\}$, where $y = \frac{1}{\beta r^{\alpha}}$.

$$\begin{aligned} p(\lambda) &= \mathbb{P}^0(Y > y) \\ &= \mathbb{P}^0(Y > y|Y_n > y)\mathbb{P}^0(Y_n > y) \\ &\quad + \mathbb{P}^0(Y > y|Y_n \leq y)\mathbb{P}^0(Y_n \leq y) \\ &= \mathbb{P}^0(Y_n > y) + \mathbb{P}^0(Y_f > y)\mathbb{P}^0(Y_n \leq y) \\ &= 1 - \mathbb{P}^0(Y_n \leq y) + \mathbb{P}^0(Y_f > y)\mathbb{P}^0(Y_f \leq y) \\ &= 1 - (1 - \mathbb{P}^0(Y_f > y))\mathbb{P}^0(Y_n \leq y) \\ &< 1 - (1 - \exp\{-\Lambda^*(F_f)\})\exp\{-\lambda\nu(F_n)\} \end{aligned} \tag{58}$$

where $\mathrm{e}^{-\Lambda^*(F_f)}$ is the Chernoff upper bound on the probability of a far-field-induced outage event. The third line is obtained from the second by recognizing that i) $\mathbb{P}^0(Y > y|Y_n > y) = 1$, and ii) $\mathbb{P}^0(Y > y|Y_n \leq y) = \mathbb{P}(Y_f > y)$ (since the events $\{Y_n \leq y\}$ and $\{Y_n = 0\}$ are equivalent). From here the remaining lines are simple rearrangements. □

References

[1] P. Gupta and P. Kumar, "Toward and information theory of large networks: An achievable rate region," *IEEE Trans. Inf. Theory*, vol. 49, no. 8, pp. 1877–1894, Aug. 2003.

[2] P. Gupta and P. Kumar, "The capacity of wireless networks," *IEEE Trans. Inf. Theory*, vol. 46, no. 2, pp. 388–404, Mar. 2000.

[3] M. Grossglauser and D. Tse, "Mobility increases the capacity of ad-hoc wireless networks," *IEEE/ACM Trans. Netw.*, vol. 10, no. 4, pp. 477–486, Aug. 2002.

[4] R. Gowaikar, B. Hochwald, and B. Hassibi, "Communication over a wireless network with random connections," *IEEE Trans. Inf. Theory*, vol. 52, no. 7, pp. 2857–2871, Jul. 2006.

[5] R. Negi and A. Rajeswaran, "Capacity of power constrained ad hoc networks," in *Proc. IEEE INFOCOM*, Hong Kong, Mar. 2004, vol. 1, pp. 443–453.

[6] L. Xie and P. R. Kumar, "A network information theory for wireless communication: Scaling laws and optimal operation," *IEEE Trans. Inf. Theory*, vol. 50, no. 5, pp. 748–767, May 2004.

[7] F. Xue, L. Xie, and P. R. Kumar, "The transport capacity of wireless networks over fading channels," *IEEE Trans. Inf. Theory*, vol. 50, no. 3, pp. 834–847, Mar. 2005.

[8] O. Leveque and İ. E. Teletar, "Information-theoretic upper bounds on the capacity of large extended ad hoc wireless networks," *IEEE Trans. Inf. Theory*, vol. 51, no. 3, pp. 858–865, Mar. 2005.

[9] F. Baccelli and S. Zuyev, "Stochastic geometry models of mobile communication networks," in *Frontiers in Queueing*. Boca Raton, FL: CRC, 1997, pp. 227–243.

[10] F. Baccelli, B. Błaszczyszyn, and P. Muhlethaler, "An Aloha protocol for multihop mobile wireless networks," *IEEE Trans. Inf. Theory*, vol. 52, no. 2, pp. 421–436, Feb. 2006.

[11] C. C. Chan and S. Hanly, "Calculating the outage probability in a CDMA network with spatial poisson traffic," *IEEE Trans. Veh. Technol.*, vol. 50, no. 1, pp. 183–204, Jan. 2001.

[12] S. Weber, X. Yang, J. G. Andrews, and G. de Veciana, "Transmission capacity of wireless ad hoc networks with outage constraints," *IEEE Trans. Inf. Theory*, vol. 51, no. 12, pp. 4091–4102, Dec. 2005.

[13] E. S. Sousa, "Performance of a spread spectrum packet radio network link in a poisson field of interferers," *IEEE Trans. Inf. Theory*, vol. 38, no. 6, pp. 1743–1754, Nov. 1992.

[14] E. S. Sousa and J. A. Silvester, "Optimum transmission ranges in a direct-sequence spread-spectrum multihop packet radio network," *IEEE J. Sel. Areas Commun.*, vol. 8, no. 5, pp. 762–771, Jun. 1990.

[15] S. Verdú, *Multiuser Detection*. Cambridge, U.K.: Cambridge Univ. Press, 1998.

[16] X. Wang and H. Poor, *Wireless Communication Systems: Advanced Techniques for Signal Reception*. Upper Saddle River, NJ: Prentice-Hall, 2003.

[17] T. Cover, "Broadcast channels," *IEEE Trans. Inf. Theory*, vol. IT-18, no. 1, pp. 2–14, Jan. 1972.

[18] J. G. Andrews, "Interference cancellation for cellular systems: A contemporary overview," *IEEE Wireless Commun.*, vol. 12, no. 2, pp. 19–29, Apr. 2005.

[19] A. J. Viterbi, "Very low rate convolutional codes for maximum theoretical performance of spread-spectrum multiple-access channels," *IEEE J. Sel. Areas Commun.*, vol. 8, no. 4, pp. 641–649, May 1990.

[20] T. Cover and J. Thomas, *Elements of information theory*. New York: Wiley, 1991.

[21] B. Rimoldi and R. Urbanke, "A rate splitting approach to the Gaussian multiple access channel," *IEEE Trans. Inf. Theory*, vol. 42, no. 2, pp. 364–375, Mar. 1996.

[22] D. N. C. Tse and P. Viswanath, *Fundamentals of Wireless Communication*. Cambridge, U.K.: Cambridge Univ. Press, 2005.

[23] S. Toumpis and A. J. Goldsmith, "Capacity regions for wireless ad hoc networks," *IEEE Trans. Wireless Commun.*, vol. 24, no. 5, pp. 736–748, May 2003.

[24] P. Patel and J. Holtzman, "Analysis of a simple successive interference cancellation scheme in a DS/CDMA system," *IEEE J. Sel. Areas Commun.*, vol. 12, no. 5, pp. 796–807, Jun. 1994.

[25] R. M. Buehrer, "Equal BER performance in linear successive interference cancellation for CDMA systems," *IEEE Trans. Commun.*, vol. 49, no. 7, pp. 1250–1258, Jul. 2001.

[26] J. G. Andrews and T. Meng, "Optimum power control for successive interference cancellation with imperfect channel estimation," *IEEE Trans. Wireless Commun.*, vol. 2, no. 2, pp. 375–383, Mar. 2003.

[27] F. Baccelli, "Stochastic Geometry: A Tool for Modeling Telecommunication Networks," INRIA-ENS, [Online]. Available: http://www.di.ens.fr/~mistral/sg/ webpage

[28] S. Weber and J. G. Andrews, "A stochastic geometry approach to wideband ad hoc networks with channel variations," in *Proc. 2nd Workshop on Spatial Stochastic Models for Wireless Networks (SPASWIN)*, Boston, MA, Apr. 2006, pp. 1–6.

[29] S. Weber and J. G. Andrews, "Bounds on the SIR distribution for a class of channel models in ad hoc networks," in *Proce. 49th Annu. IEEE Globecom Conf.*, San Francisco, CA, Nov. 2006, pp. 1–5.

[30] W. Schottky, "Uber spontane stromschwankungen in verschiedenen elektrizitatsleitern," *Ann. der Physik*, vol. 57, pp. 541–567, 1918.

[31] S. B. Lowen and M. C. Teich, "Power-law shot noise," *IEEE Trans. Inf. Theory*, vol. 36, no. 6, pp. 1302–1318, Nov. 1990.

[32] D. Stoyan, W. Kendall, and J. Mecke, *Stochastic Geometry and Its Applications*, 2nd ed. New York: Wiley, 1996.

[33] D. Warrier and U. Madhow, "On the capacity of cellular CDMA with successive decoding and controlled power disparities," in *Proc. IEEE Vehicular Technology Conf.*, Ottawa, ON, Canada, May 1998, pp. 1873–1877.

[34] D. Stoyan and H. Stoyan, *Fractals, Random Shapes, and Point Fields*. New York: Wiley, 1994.